Kinetics and thermodynamics of end-functionalized polymer adsorption and desorption processes

Richard Zajac and Amitabha Chakrabarti
Department of Physics, Kansas State University, Manhattan, Kansas 66506
(Received 25 October 1993)

We present results from a Monte Carlo study of adsorption processes of end-functionalized polymers from a solution to an adsorbing solid surface. We consider moderately large polymer chains with up to 200 monomers, and study the kinetics of polymer brush formation in a situation where the brush is in contact with a bulk reservoir which can supply chains to the brush without any limit. In our simulations, we consider both the kinetics of the adsorption process and the equilibrium structure of the brushes thus formed. Once the brushes are formed and in equilibrium, we study the desorption of such an equilibrium brush layer under the conditions of (i) rinsing by a pure solvent, and (ii) keeping the brush in contact with a solution containing other "attacking" chains with either stronger functional groups or shorter lengths. The results of these studies are compared with analytical theories and experiments.

PACS number(s): 61.25.Hq

I. INTRODUCTION

The use of polymers in controlling the aggregation properties of colloidal systems is important in a wide range of areas such as paints, glues, food emulsion, pharmaceuticals, etc. In such cases, a dispersed system in which colloidal particles are maintained in suspension is desired. This stabilization can be achieved by end grafting suitable polymer chains to the surfaces of the colloidal particles [1,2]. In an ideal situation, the repulsion between the resulting polymer layers or "brushes" [3,4] maintains the colloidal particles at distances great enough to render the inherent attractive forces insignificant. The response of a brush upon coming into contact with another brush [5] depends on the details of the chain configurations in the brushes. A proper theoretical understanding of the stabilization process thus requires a thorough knowledge of the structure of the polymer brush in various solvent conditions and in the presence of various surface interactions. An important step toward this has been taken recently by developing a self-consistent-field (SCF) formulation [6–9] for a polymer brush. The SCF theory of Milner, Witten, and Cates (MWC) [7] predicts that for good solvent conditions and moderately high grafting densities, the density profile should be of a parabolic shape, in contrast to the step-function profile assumed by Alexander [10] and de Gennes [11]. This parabolic density profile has been observed in previous computer simulations [12–14] and in some recent experiments [15–17].

Most of these previous studies have considered polymer brushes with a preassigned surface coverage, and have assumed that the end-grafted functional groups are never detached from the grafting surface. Thus, no exchange of polymer chains between the grafted layer and the solution forming the brush has been allowed in the above studies. In most of the experimental situations, on the other hand, the grafted layer is constructed by keeping a solution of end-functionalized polymers in contact with an adsorbing surface. In these cases, then, the monomer concentration of the bulk solution is kept fixed, and the adsorbed polymer layer is allowed to form by self-assembly of the functionalized polymer chains at the adsorbing wall. The final equilibrium state of the adsorbed layer is then governed by the reversible exchange of polymer chains between the grafted layer and the solution. The kinetics of formation of such a grafted layer and the thermodynamics of the equilibrium layer thus formed have been receiving attention only recently. Analytical studies of the process of the brush formation and the subsequent desorption of the polymers under various conditions have been carried out by Ligoure and Leibler (LL) [18] and by Milner [19]. Computer simulations have also been carried out recently by Lai [20], where chain exchange with the bulk solution was allowed. However, the chains in this simulation study were too short for any meaningful comparison with theoretical predictions.

In this paper, we report results from an extensive Monte Carlo simulation of the brush formation (and subsequent desorption) from solutions. We study chains with up to 200 monomers (chain length $N=199$) which is an order of magnitude larger than the maximum chain length used by Lai. Moreover, by averaging over many initial conditions we are able to study the kinetics of the brush formation quite accurately. We should also point out that instead of using a closed system with a fixed number of chains (as used by Lai), we consider the situation where the brush is in contact with a bulk reservoir which can supply chains to the brush without any limit. This is the condition under which the theoretical results are strictly valid, and thus a quantitative comparison with the theoretical prediction is possible with the results of our simulation. Besides, considering a closed system with a finite size is more prone to finite-size effects, as already recognized by Lai. In our simulation we consider both the kinetics of the adsorption process and the equilibrium structure of the brushes thus formed. Once the

brushes are formed and are in equilibrium, we study the desorption of such an equilibrium brush layer under the condition of rinsing by a pure solvent, and also when the brush is kept in contact with other "attacking" chains, with either stronger functional groups or shorter lengths.

We organize the rest of the paper as follows. In Sec. II, we describe the model used and the method of simulation used in this study. In Sec. III we present results for thermodynamics and the kinetics of adsorption processes. This section is divided into two parts. In Sec. III A, we present the results from the kinetics part during the formation of the brush, and in Sec. III B, we present results from the analysis of the structure of the brush layer in equilibrium. In Sec. IV, we present results of the desorption process under various solution conditions. This section is also divided into two subsections. In Sec. IV A, we present results from studies of rinsing of the brush layer with pure solvents, and in the subsequent Sec. IV B, we present results from studies where the equilibrated brushes are in contact of solution of polymer chains with either more strongly adsorbing end groups or shorter lengths. The results of these studies are compared with analytical theories and experiments wherever possible. In Sec. V, we give a summary of the main results and a brief conclusion.

II. SIMULATION METHODS

In this section, we describe the general Monte Carlo simulation methods [21] used to implement movements of the chains. The details of the simulation technique are different for different sets of calculations and those particular details are described separately in later sections. We model the polymer chains as N-step self-avoiding random walks on a three dimensional $50\times50\times100$ cubic lattice, with the first monomer of each chain representing an adsorbing functional group ("sticker"). Periodic boundary conditions are applied in the x and y directions, and the system is bounded in the z direction by two impenetrable surfaces at $z=0$ and $z=99$. The surface at $z=0$ is the only adsorbing surface, while the other surface at $z=99$ is noninteracting. The wall-wall distance is much larger than both the typical size of the chains in the solution, and the expected brush height. Thus, the second surface should not affect the adsorption process. This was explicitly checked in some trial runs. A number N_c of polymer chains is randomly placed on the lattice to make up the desired bulk concentration of monomers (ϕ_0). The chains are placed one at a time, with care taken to avoid any site which is already occupied. Lattice sites which are not occupied by monomers represent solvent molecules. The evolution of the chains is performed according to Monte Carlo criteria, whereby a monomer is chosen at random and an arbitrary move is attempted about it. These moves consist of kink jumps, crankshaft turns, and a slithering-snake-type motion (loosely called a "reptation" move) [21], weighted so that half of the attempted moves are reptations. A move is rejected if it requires the chain to migrate to any lattice site already occupied by a monomer. In this way, the chains interact via the excluded volume interaction. We measure time by the number of moves that are attempted. In this way, one Monte Carlo step per monomer (MCS/M) is defined as $N\times N_c$ attempted moves, corresponding to one attempted move on the average for each monomer in the system. Since the monomers are chosen in a random fashion, it is possible that some of the monomers may not be selected for an attempted move. On average, however, each segment undergoes one attempted move in one MCS. The evolution of the system toward equilibrium is then repeated several times with different initial conditions, and the results of the kinetics section are then averaged over all the "runs" (typically, ten runs per system configuration).

III. THERMODYNAMICS AND KINETICS OF ADSORPTION

A. Adsorption kinetics of end-functionalized polymers

After starting from an initial random configuration for the polymer chains with a given monomer concentration (ϕ_0), the chains are equilibrated at an infinite temperature for about 1000 MCS/M. Subsequently, the interaction with the end-functional group and the adsorbing surface is "turned on," so that absorption of the "sticker" to the impenetrable surface at $z=0$ becomes energetically favored. Then, any move consistent with the excluded-volume criterion, which requires a sticker to become detached from this adsorbing surface, is accepted with the probability $e^{-\Delta}$, where Δ is the energy gained (in units of kT) by the sticker in adsorbing to the surface. This adsorption energy leads to the formation of an adsorbed "brush" layer at the surface, which would progressively deplete the system of its free chains. In order to maintain a constant monomer density far from the surface, every time a chain gets adsorbed we attempt to place a new chain on the lattice at some random location [22]. If the attempt fails, we try again with a new randomly chosen location. Thus, the ease with which a chain is introduced in the system depends on the monomer concentration around that location. Similarly, for each chain which becomes desorbed, we select a free chain at random and delete it from the lattice. In this way, we are considering that the system is connected to a reservoir so that the total number of chains can continually change to maintain a constant chain density in the bulk. In practice, the total number of chains is adjusted every 10 MCS/M, to avoid repeatedly adding and deleting chains as a sticker fluctuates about the surface.

We investigate the kinetics of this adsorption process for systems with $\Delta=6$ and 9. For the $\Delta=6$ systems, we consider a bulk monomer concentration of 5% for chain lengths $N=49$ and 99. We also consider systems with $\Delta=9$ and a bulk monomer concentration of 2.5%, for chain lengths of $N=49$, 99, and 199. The solution conditions from which chains are being adsorbed are in the semidilute range for the chain lengths considered. In Figs. 1(a)–1(c) we show the evolution of the system with time for a typical run. The number of polymer chains adsorbed per unit area $\sigma(t)$ increases with time (t), until the

system finally reaches equilibrium and the number of polymer chains adsorbed starts fluctuating about the equilibrium value σ_{eq}. In Figs. 2(a) and 2(b) we show log-log plots of $\sigma(t)$ vs t for two different values of Δ and various chain lengths. In all the cases studied here, we find that $\sigma(t) \sim t^{1/2}$ in the early to intermediate stages of the evolution process. This is consistent with the prediction [18] that at early times the kinetics of the adsorption process is governed by Brownian diffusion of the chains in the solution. The long-time dynamics of the adsorption process is expected to be controlled by the activation barrier, created by the polymer chains belonging to the brush, against new chains being adsorbed to the surface [18,19]. In this regime $\sigma(t)$ would increase logarithmically with time t. This logarithmic behavior in the case of a strongly stretched adsorbed layer arises due to the fact that an adsorbing chain would have to give up some of its free energy to introduce itself into the brush. This activation barrier may not be very strong in the simulations since, as we will present shortly, the polymer chains in the brushes are not strongly stretched for the cases considered here. This may be due to the fact that the chain lengths used in the simulations are not large enough to produce strongly stretched brushes. However, we note that there is some evidence of slow kinetics in the simulation near equilibrium, where we find that the evolution is slower than that in the earlier stages.

We now present the evolution of the density profile for the adsorbed chains. In Fig. 3(a) we plot the density profile $\phi(z,t)$ vs z for $N=99$ and $\Delta=6$, for various times. In Fig. 3(b) we carry out a dynamical scaling analysis of

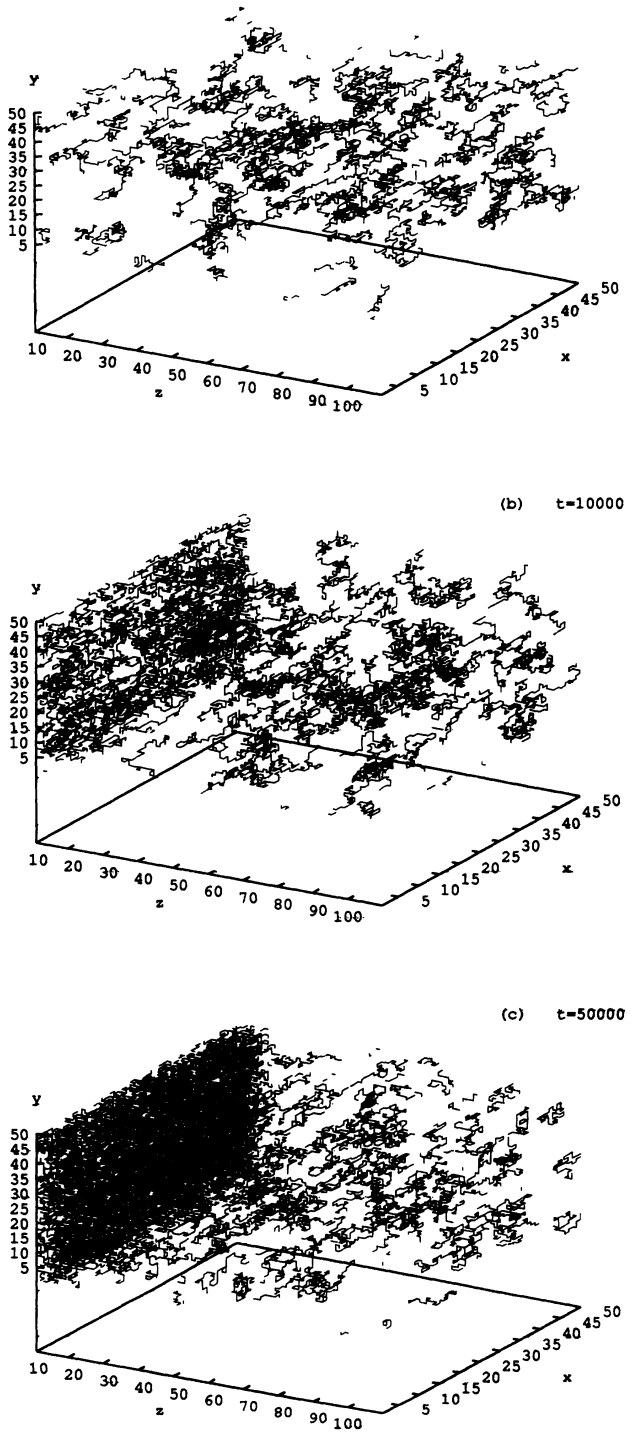

FIG. 1. (a) A typical configuration of the system at time $t=0$. Here the chain length $N=49$, adsorption strength $\Delta=6$, and bulk monomer density $\phi_0=5\%$. (b) Same as in (a) except for $t=10000$ MCS/M. Note the buildup of the adsorbed layer. (c) Same as in (b) except for $t=50000$ MCS/M. By this time the system has reached equilibrium.

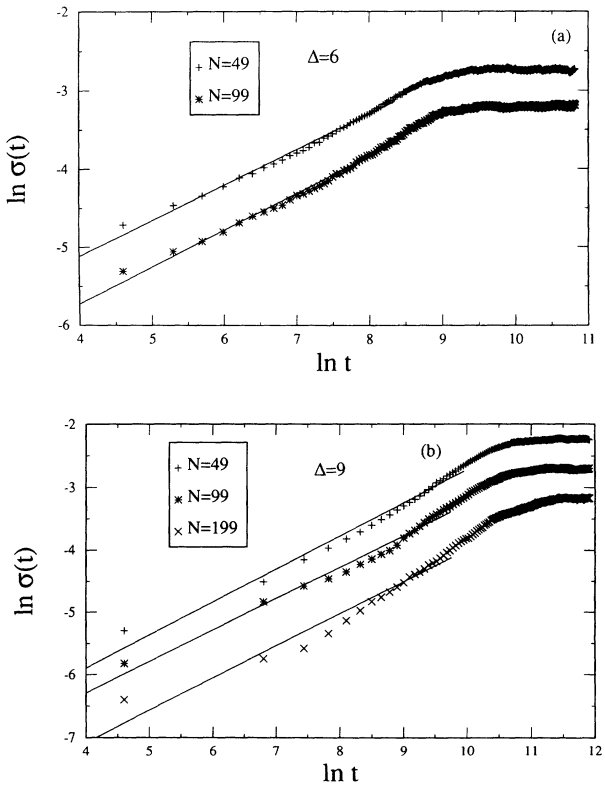

FIG. 2. (a) Log-log plot of the number of chains adsorbed per unit area (surface coverage of adsorbed chains) $\sigma(t)$ vs t for $\Delta=6$ and for $N=49$ and 99. The slopes of the straight lines are 0.51 and 0.49, respectively. (b) Same as in (a) except for $\Delta=9$. Here $N=49$, $N=99$, and $N=199$. The slopes of the straight lines are 0.53, 0.52, and 0.52, respectively.

these profiles by rescaling z by $\langle z(t)\rangle$ and $\phi(z,t)$ by $\phi_{\max}(t)$, where $\langle z(t)\rangle$ is the first moment of the density profile (which should be a reasonably good measure of the brush height), and $\phi_{\max}(t)$ is the maximum value of the density profile (note that in the simulation this maximum in the density profile does not occur right at the surface; rather the maximum is located at a distance of a few monomer sizes away from the adsorbing surface). At late times, scaling works quite well in this form, indicating that the layer height is the dominant length scale during the adsorption process. Similar scaling plots can be obtained for other values of N and Δ.

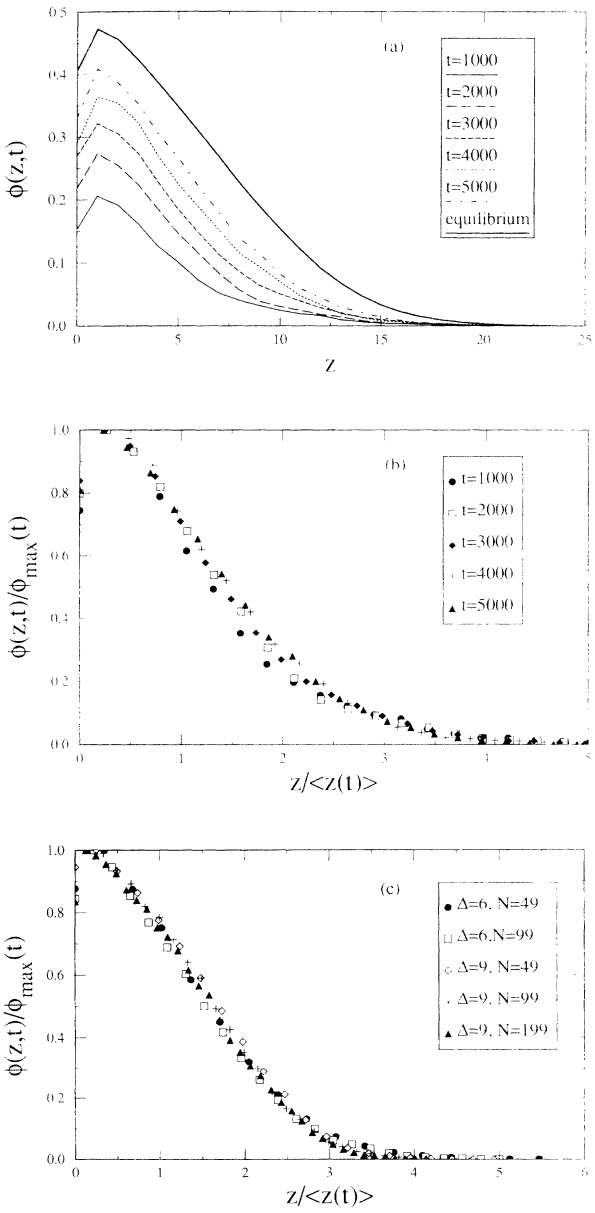

FIG. 3. (a) The density profile of the adsorbed layer at various times. Here $\Delta=6$ and $N=99$. The density profile at equilibrium is also shown for comparison. (b) Dynamical scaling plot of the normalized density profiles shown in (a). (b) Dynamical scaling plot of the normalized density profiles for various N and Δ values. Here the data correspond to $t\approx\tau_{\rm eq}/2$.

We compute various time scales associated with the construction of the brush layer. One such time scale is the equilibration time $\tau_{\rm eq}$, which is the time required to reach equilibrium, as computed from the plateau of the $\sigma(t)$ curves. We also compute another time scale τ_c, which is a measure of the time required to construct the brush layer in the following way. First we define a quantity,

$$\bar{\sigma}(t)=[\sigma(t)-\sigma_{\rm eq}]/\sigma_{\rm eq}\ , \tag{1}$$

and then define τ_c as the integral,

$$\tau_c=-\int_0^\infty \bar{\sigma}(t)dt\ . \tag{2}$$

The time scales $\tau_{\rm eq}$ and τ_c are listed in Table I.

In Fig. 3(c) we show another scaling plot with data taken from runs with various values of N and Δ. We choose $t\approx\tau_{\rm eq}/2$ in each case. We carry out a scaling analysis similar to that of Fig. 3(b), and find that scaling again works reasonably well, indicating that the kinetics of the adsorption process for various N and Δ values can be understood in terms of a dominant length scale, namely the brush height.

B. Equilibrium structure of the grafted layer

In Table II we list various properties of the adsorbed layer at equilibrium. Before we analyze the equilibrium data, let us first point out that we have checked that proper equilibrium has been obtained by starting from two very different initial configurations. One such case is shown in Fig. 4 for $N=49$ and $\Delta=9$, where we show the evolution of the system for two initial configurations, one with no adsorbed chains at the beginning, and the other starting with about twice as many chains as can be adsorbed to the surface in equilibrium. The fact that the evolution of the system converges to a state with the same number of chains adsorbed gives us confidence that the data presented in Table II correspond to the true equilibrium situation.

Typical equilibrium density profiles of adsorbed and free chain monomers are shown in Figs. 5(a) and 5(b). It is quite clear that the adsorbed profile is nonparabolic. We empirically find that the profile resembles a Gaussian form, i.e., $\phi_{\rm eq}(z)=Ae^{-Bz^2}$, although we do not know of any theoretical work which predicts a Gaussian density profile for grafted polymers. The fitting parameters for these Gaussian fits are listed in Table III. We believe that this nonparabolic behavior is due to the presence of

TABLE I. Characteristic time scales (in units of MCS/M) $\tau_{\rm eq}$ and τ_c (see text) corresponding to the construction of the grafted brush layer from the solution.

N	Δ	ϕ_0	$\tau_{\rm eq}$	τ_c
49	6	0.0535	8 100	3 500
99	6	0.0551	13 400	4 000
49	9	0.0277	60 000	18 500
99	9	0.0294	77 000	18 800
199	9	0.0313	98 000	27 100

TABLE II. Characteristics of the adsorbed brush layer in equilibrium. The unperturbed radius of the chains $\bar{R}_e$ are computed from the relation $\bar{R}_e = aN^{\nu}$, where we have put $\nu = 0.6$ and $a = 1$, consistent with the results of Monte Carlo simulations of lattice chains in Ref. [23].

N	Δ	ϕ_0	σ_{eq}	$\langle z_{eq} \rangle$	ϕ_{eq} $(z=0)$	ϕ_{max}	R_e	$\bar{R}_e$	$R_\perp$	$\frac{R_\perp}{\sigma_{eq}^{1/3}}$	ω
49	6	0.0535	0.065	4.44	0.47	0.51	20.55	10.33	5.71	14.2	0.28
99	6	0.0551	0.041	5.31	0.41	0.47	26.00	15.75	8.27	24.1	0.18
49	9	0.0277	0.107	5.45	0.60	0.63	21.06	10.33	7.68	16.2	0.27
99	9	0.0294	0.067	6.23	0.52	0.57	25.44	15.75	11.40	28.1	0.17
199	9	0.0313	0.042	7.50	0.45	0.53	31.24	23.95	17.02	49.0	0.11

the free chains which penetrate into the brush layer to some extent. The adsorbed chains are not strongly stretched, due to the screening effect produced by the free chains, and this may account for the nonparabolic behavior of the density profile. Indeed, if we instantaneously remove all free chains from the system, we find that the adsorption profile quickly (within a few hundred MCS/M) assumes a parabolic form. Averaging over all chains in equilibrium, we measure the end-to-end length of a chain R_e in the brush layer. By comparing R_e in the brush layer with the corresponding end-to-end distance of free, unperturbed chains ($\bar{R}_e$) [23] (see Table II), we conclude that the adsorbed chains are not strongly stretched. It seems that much longer chain lengths and stronger adsorption strength are necessary to get a strongly stretched brush layer. As an indicator of the extent to which the chains are stretched in the brush layer, and as a measure of the brush height, we compute the *perpendicular* end-to-end distance of the adsorbed chains $R_\perp$. The corresponding rescaled quantity $R_\perp/\sigma_{eq}^{1/3}$ in equilibrium is tabulated in Table II in each case. In the strongly stretched regime the above ratio should scale as N; here, however, we find that $R_\perp/\sigma_{eq}^{1/3} \approx N^{0.78}$. This again indicates that the adsorbed chains are not strongly stretched.

The equilibrium density profiles for various N and Δ values are shown in Fig. 6 in a scaling plot, where we plot the rescaled density $\phi_{eq}(z)/\phi_{max}$ vs the rescaled distance $z/\langle z_{eq} \rangle$. From this plot, we conclude that the scaling description also works well at equilibrium. We have also compared the profiles to those obtained from a Scheutjens-Fleer-type numerical self-consistent-field (SCF) model [24], adapted to the conditions of our Monte Carlo model. Considering values of the Flory-Huggins parameter to be $\chi = 0$ (self-avoiding walk) and $\chi = 0.5$ (random walk), we have found that although the SCF model yields the same qualitative shape for the density profile, it grossly underestimates the amount of adsorbed polymer. In fact, the SCF results would seem to indicate that a negative (unphysical) value of χ is required to represent this many-body problem. This would imply that the interaction between adsorbed chains, beyond being screened out, actually becomes attractive.

The assumption of a parabolic profile serves as a starting point for some previous studies of the adsorption

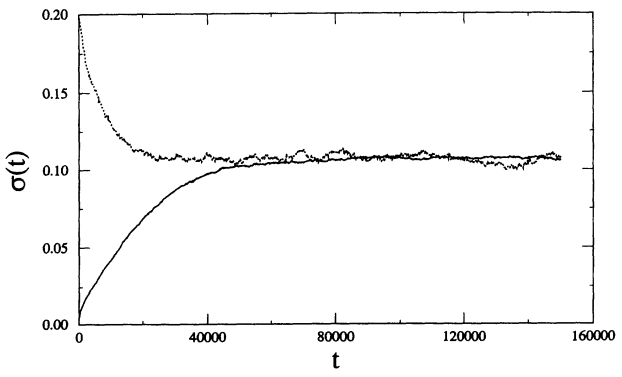

FIG. 4. Test of equilibrium for a run with $N = 49$ and $\Delta = 9$. The two lines correspond to two different initial conditions: one with no chains adsorbed initially, and the other one with a very large number of chains adsorbed at the surface.

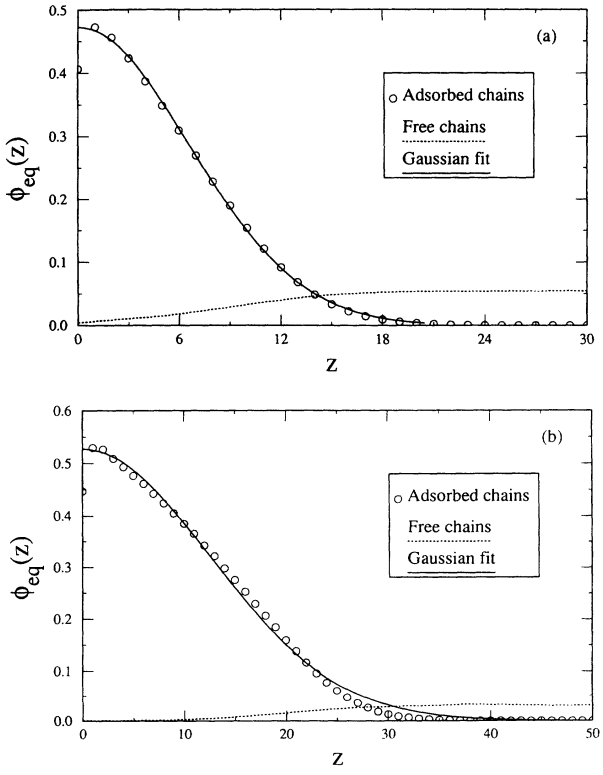

FIG. 5. (a) Equilibrium density profiles for the adsorbed and the free chains. Here $N = 99$ and $\Delta = 6$. The solid line is a fit to a Gaussian profile. (b) Same as in (a) except for $N = 199$ and $\Delta = 9$ in this case.

TABLE III. Fitting parameters A and B computed from fitting the equilibrium density profiles of the brushes to an empirical Gaussian form $\phi_{eq}(z)=Ae^{-Bz^2}$.

N	Δ	ϕ_0	σ_{eq}	A	B
49	6	0.0535	0.065	0.516	0.022 61
99	6	0.0551	0.041	0.472	0.011 47
49	9	0.0277	0.107	0.639	0.011 96
99	9	0.0294	0.067	0.574	0.006 00
199	9	0.0313	0.042	0.527	0.003 13

kinetics [18–19]. This assumption, which corresponds to the limit of strongly stretched chains, turns out to be inapplicable to the systems we are considering, as a parabolic profile cannot be attained in this regime. As has been discussed by Ligoure and Leibler and by Milner, the final equilibrium surface coverage σ_{eq} for a bare surface growing a brush from solution would be governed by the reversible exchange of chains from solution. After matching different energy and entropy contributions, one can write the equilibrium condition as

$$f-\Delta+\ln\sigma_{eq}=\ln\phi_0 , \tag{3}$$

where f is the free energy per chain in the brush relative to a coil in the solution. LL and Milner then assume that the chains are strongly stretched in the adsorbed layer and write

$$f=3/2(\pi^2/12)^{1/3}N\sigma_{eq}^{2/3} . \tag{4}$$

By solving Eqs. (1) and (2), one can then obtain σ_{eq} for various values of N and Δ. This will not be particularly useful in our case, since we cannot use the expression for f given in Eq. (2), which is valid only in the strongly stretched regime.

LL write Eq. (1) in another equivalent way as

$$N\omega\phi_0\alpha=\Delta+\ln(\phi_0/\alpha) , \tag{5}$$

where $\alpha=[\phi_{eq}(z=0)-\phi_0]/\phi_0$, and ω is the *(effective)* value of the excluded-volume parameter. This effective value of ω is expected to be different in the presence of the free chains, due to the screening effect produced by these free chains. From the above equation, we compute this effective value of ω and tabulate it in Table II as well. Note that these values of ω are *considerably less* than the value ($\omega=0.5$) obtained in the previous Monte Carlo simulation of a strongly stretched grafted polymer brush in good solvent condition yielding a parabolic density profile [12a]. This decrease of the excluded-volume parameter is the reason why the grafted layer is not strongly stretched in the present simulation. Our results for the effective value of ω suggest that ω depends only on N. To understand the result, one needs to consider a polymer brush kept in contact with a matrix of polymer chains of length P. This problem has been considered by several authors [25–29] before. In such a situation, one can show that the expression for the brush height can alternatively be written in terms of an effective excluded volume parameter which goes as P^{-1}. Since in our case, the free chains are of the same length as the adsorbed chains; $P=N$, and we expect that the effective $\omega\sim N^{-1}$. Since we have data for very limited ranges of N values, it is very difficult to extract the N dependence of the effective value of ω. From the few data points we have, we find that $\omega\approx N^{-3/4}$ or so.

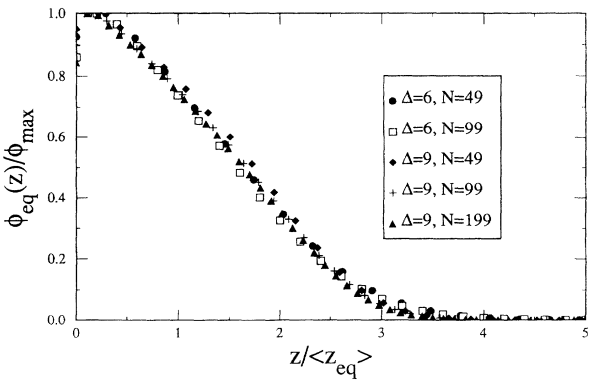

FIG. 6. Scaling plot of the normalized equilibrium density profiles for various N and Δ values.

IV. DESORPTION KINETICS OF THE GRAFTED LAYER

A. Rinsing of the brush layer with pure solvents

We next investigate the behavior of an adsorbed brush layer being rinsed away by immersion in a pure solvent. The equilibrium chain configuration from Sec. III B is used to provide the brush layer by keeping only those chains whose stickers are on the adsorbing surface. To this end, the free chains are removed from the system, which is equivalent to placing the surface and the adsorbed layer in a pure solvent. The chains are then allowed to evolve according to the same criteria as before. We consider two cases: (a) a closed system, such that desorbing chains are allowed to remain in the bulk phase; (b) an open system, such that desorbing chains are deleted ("flushed away") from the system when they are completely past the furthest extent of the brush layer, which also evolves dynamically. In the first case, the total number of chains in the whole system remains constant. The second case corresponds to a very large reservoir of solvent with a current which removes the desorbed chains once they are clear of the brush.

We consider such rinses for the $\Delta=6$ systems for both $N=49$ and $N=99$. For both $N=49$ and $N=99$, the decrease of $\sigma(t)$ with time for the closed system is plotted in Fig. 7(a). In this case, we note that $\sigma(t)$ decreases initially, and eventually reaches a new equilibrium, as the desorbed chains build up a new bulk monomer concentration. The corresponding decrease of $\sigma(t)$ for the second case, i.e., an open system, is seen to decrease exponentially in the semilog plot of Fig. 7(b), as predicted by LL [18]. By fitting this decay to a functional form

$$\sigma(t)=Ae^{-t/\tau_{w_1}} , \tag{6}$$

we compute the time constant τ_{w_1} associated with this

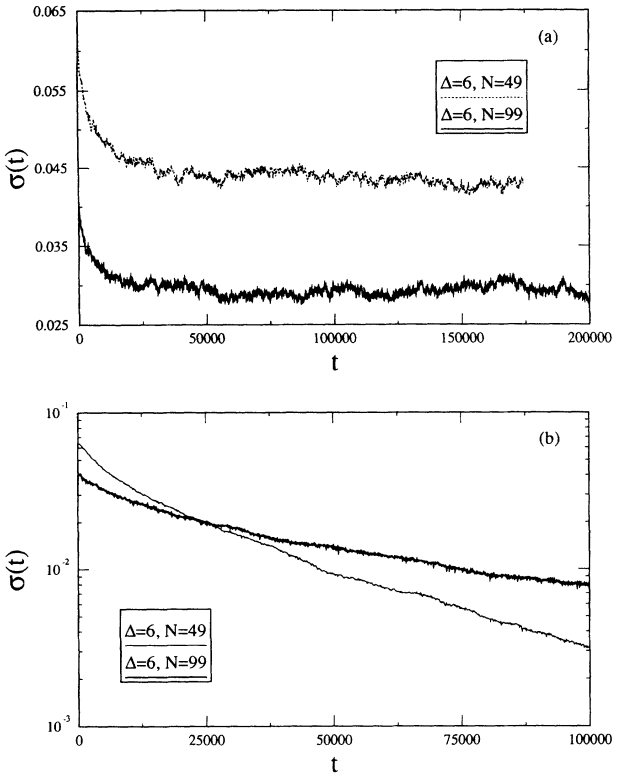

FIG. 7. (a) Decay of the number of adsorbed chains per unit area (surface coverage) $\sigma(t)$ with time t for a rinse with pure solvent in a closed system. Here $N=49$ and $N=99$, respectively, and $\Delta=6$. (b) Semilog plot of the decay of the surface coverage $\sigma(t)$ with time t for a rinse with pure solvent in an open system. Here $N=49$ and $N=99$, respectively, and $\Delta=6$.

wash. These values of τ_{w_1} for two different N values are listed in Table IV. We also extract a time scale for the closed-system wash τ_{w_2} in the following way. For this purpose, we first define a quantity,

$$\bar{\sigma}(t)=[\sigma(t)-\sigma_{eq}]/(\sigma_0-\sigma_{eq}) \tag{7}$$

and then define τ_{w_2} as the integral,

$$\tau_{w_2}=\int_0^\infty \bar{\sigma}(t)dt \ . \tag{8}$$

This time scale τ_{w_2} is also listed in Table IV. Note that these values of the characteristic time associated with the desorption of the brush are *much longer* than the corresponding characteristic times for the construction of the brush (which are listed in Table II). This result is in good agreement with the theoretical predictions of LL.

TABLE IV. Characteristic time scales (in units of MCS/M) corresponding to the desorption of the grafted brush layer for a rinse with the pure solvent under open-system and closed-system conditions.

N	Δ	τ_{w_1}	τ_{w_2}
49	6	39 800	13 900
99	6	71 500	19 900

B. Competitive adsorption

We consider the effect of placing an adsorbed polymer brush (A phase) in a solution of unlike polymer (B phase), with the intent to actively remove and replace the brush polymer. We again consider two cases: (a) replacement by chains of similar molecular weight but stronger adsorption energy; (b) replacement by chains of smaller molecular weight but identical adsorption energy. In either case, we again start with the equilibrium configuration of part A, keeping only the adsorbed chains. We then place on the lattice an appropriate number of B-type chains such that the bulk monomer concentration of B chains is identical to what was used to form the brush layer. The B chains are initially restricted from the brush layer, corresponding to a dividing plate separating the two phases. Since the B chains are not initially distributed over the whole lattice but are confined to a portion of it away from the brush layer, the bulk concentration of B monomers is slightly higher than the desired concentration. The B chains are allowed to equilibrate for a period, after which the partition is removed. The B chains are then allowed to penetrate into the brush layer, and the A chains are also allowed to evolve. In either case, we consider only closed systems such that the total numbers of A and B chains remain constant. Desorbed chains remain in the bulk and are not deleted. It is worth noting that even in the case where the chains do not all have the same molecular weight, each monomer of every chain stands an equal chance of being selected for an attempted move. Let us first show the evolution of the density profiles for the brush layer and the initially free "attacking" polymers. As shown in Figs. 8(a) and 8(b), the brush layer desorbs in each case, while the attacking polymers slowly form an adsorbed layer. Subsequently, the system comes to equilibrium.

Now, we concentrate on the first case, where we consider replacement of a $\Delta=6$ brush with chains whose adsorption energy is $\Delta=9$. Both $N=49$ and 99 situations are considered. Equilibrium density profiles of A- and B-type chains are shown in Fig. 9(a), while coverages are plotted as functions of time in Fig. 9(b). We find that the adsorption profile of the A chains has a parabolic form, while that of the B chains has a Gaussian form. We also find that the decay of the coverage $\sigma(t)$ of the A chains can be fitted to an exponential form reasonably well, if we subtract the final equilibrium value of the surface coverage from $\sigma(t)$. We extract a time scale associated with this competitive adsorption (τ_{a_1}) in the same way as before, by defining a quantity $\bar{\sigma}(t)$ and computing the integral of this quantity. The values of the time scale τ_{a_1} are listed in Table V. Comparing this time scale with the corresponding time scale of rinsing (τ_{w_2}) with a pure solvent (in the closed system), we find that these two time scales are of similar magnitude. This indicates that the strongly adsorbing attacking chains are not very effective in displacing the adsorbed polymer brush layer. This result is in good qualitative agreement with the theoretical prediction of Milner, although the chains in our adsorbed layer are not strongly stretched.

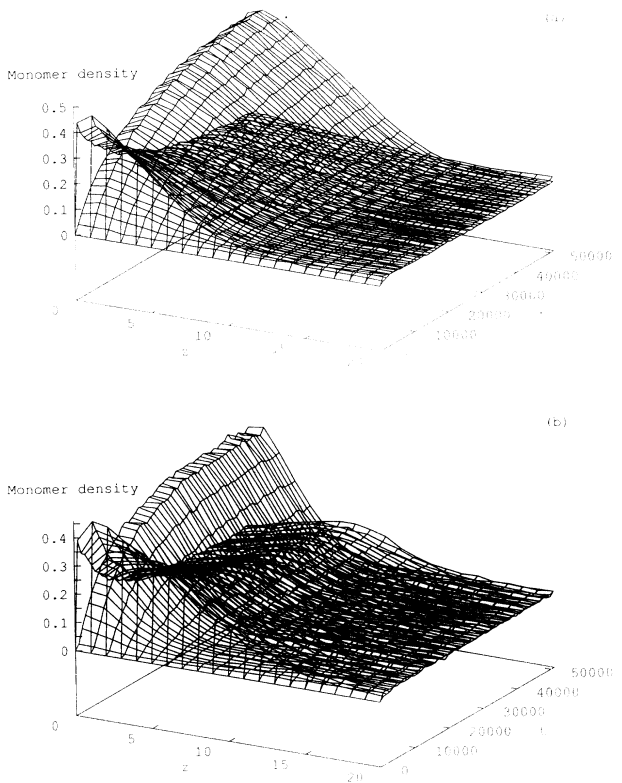

FIG. 8. (a) Competitive adsorption: Decay of the density profile for a brush layer (with $N=49$ and $\Delta=6$) and the corresponding growth of the density profile for the "attacking" chains ($N=49$, $\Delta=9$) with time. (b) Competitive adsorption: Decay of the density profile for a brush layer (with $N=99$ and $\Delta=6$) and the corresponding growth of the density profile for the "attacking" chains ($N=24$, $\Delta=6$) with time.

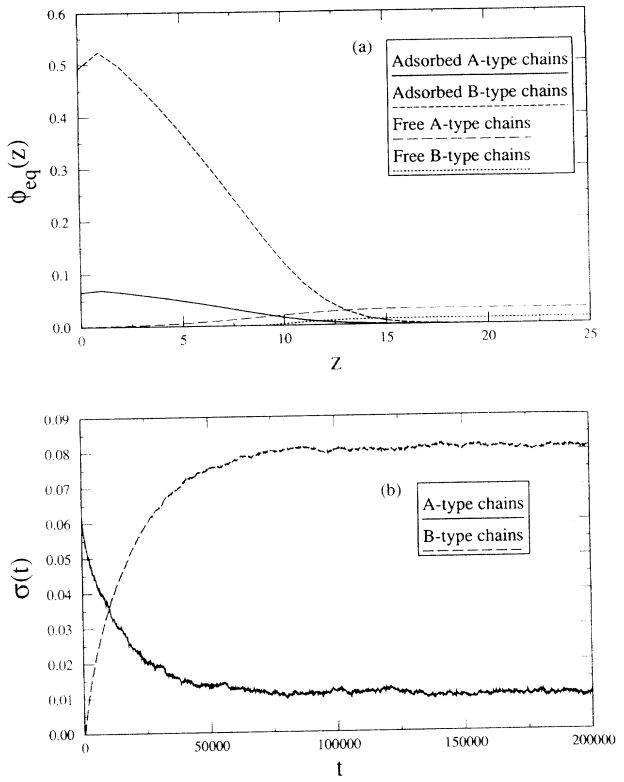

FIG. 9. (a) Equilibrium density profile under competitive adsorption. Here the A-type chains correspond to $N=49$ and $\Delta=6$; and the B-type chains correspond to $N=49$, $\Delta=9$. (b) Decay of the surface coverage for the A-type chains and the corresponding growth of the surface coverage of the B-type chains under competitive adsorption. Here the A-type chains correspond to $N=49$ and $\Delta=6$; and the B-type chains correspond to $N=49$, $\Delta=9$.

For the second case (different molecular weights), we consider the replacement of a brush with $N=49$ by chains with $N=24$ followed by the replacement of an $N=99$ brush with $N=49$ and 24 chains. In all three cases, we have $\Delta=6$. Again, equilibrium density profiles of A- and B-type chains are shown in Fig. 10(a), while coverages are plotted as functions of time in Fig. 10(b). Again, we find that the A chains' decay follows an exponential form, once the equilibrium surface coverage is subtracted out. Also, at equilibrium, the density profile for the longer chains assumes a parabolic form beyond the region dominated by the short chains. As in the previous section, we extract the time scales associated with this competitive adsorption (τ_{a_2}) and list them in Table V. Comparing this time scale with both the time scale of rinsing (τ_{w_2}) with a pure solvent (in the closed system), and with the time scale of replacing the adsorbed layers by invading polymers with the same molecular weight but strongly adsorbing sticker sites (τ_{a_1}), we find that this new time scale is smaller than both of these previously computed time scales. Thus, our results strongly indicate that shorter chains are more effective in displacing the adsorbed layer. This result is also in good qualitative agreement with the theoretical prediction of Milner, and with experimental observations [30,31]. Since we have data for only a few chain lengths, it is difficult to extract information as to how the new time scale τ_{a_2} depends on the ratio of N_A/N_B. Theoretical work of Milner predicts that the time scale for desorption by shorter chains should be reduced by a factor of $(N_A/N_B)^{-1/2}$ compared to the time scales of desorption with either pure solvent or of desorption with chains of the same molecular weight but strongly adsorbing sticker sites. Although we

TABLE V. Characteristic time scales (in units of MCS/M) corresponding to the desorption of the grafted brush layer under competitive adsorptions. Here $N_A=N$ is the chain length of the initially adsorbed polymers, and N_B and Δ_B are, respectively, the chain length and sticker adsorption energy for the "attacking" polymers.

N_A	Δ	N_B	Δ_B	τ_{a_1}	τ_{a_2}
49	6	49	9	15 600	
99	6	99	9	19 800	
49	6	24	6		10 500
99	6	24	6		11 800
99	6	49	6		13 700

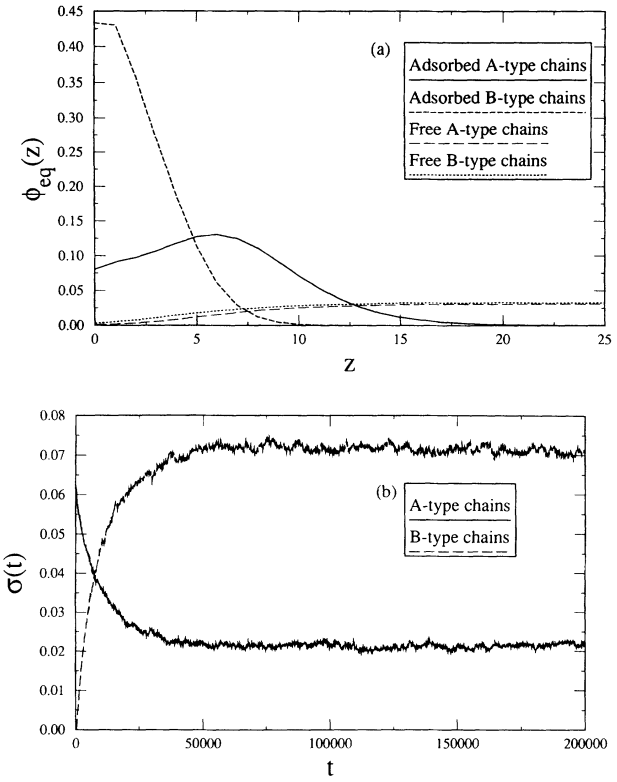

FIG. 10. (a) Equilibrium density profile under competitive adsorption. Here the A- type chains correspond to $N=99$ and $\Delta=6$; and the B-type chains correspond to $N=24$, $\Delta=6$. (b) Decay of the surface coverage for the A-type chains and the corresponding growth of the surface coverage of the B-type chains under competitive adsorption. Here the A-type chains correspond to $N=99$ and $\Delta=6$, and the B-type chains correspond to $N=24$, $\Delta=6$.

consider a closed system here, and our chains lengths are quite short for this type of theory to be applicable, we note that our data are still consistent with Milner's predictions.

V. CONCLUSIONS

Through Monte Carlo simulations of end-functionalized polymer chains in solution, we have studied the adsorption and desorption processes of polymers at a surface. We have studied the kinetics of polymer brush formation in a situation where the brush is in contact with a bulk reservoir which can supply chains to the brush without any limit. We have found that the surface coverage grows as $\sigma \sim t^{1/2}$, forming a brush layer in equilibrium with the solution. This equilibrium state is characterized by a Gaussian density profile, unlike the parabolic profiles seen in previous studies. This is due to the screening of the excluded-volume parameter provided by the significant penetration of free chains into the brush layer. The adsorbed chains are therefore not strongly stretched. We have also found that both the dynamical and equilibrium situations fit a scaling form in which the dominant length scale is given by the first moment of the density profile.

The characteristic rinsing time of this equilibrium brush layer by a pure solvent is found to be larger than the construction time, in good agreement with the predictions of Ligoure and Leibler. When the brush is immersed in a solution of different polymer chains, the time scale of its desorption is found to be smaller for a solution of shorter chains than it is for a solution of chains with greater adsorption energy. Shorter chains are thus found to be more effective than chains with a stronger functional group in displacing the brush layer. This result is in good agreement with the theoretical prediction of Milner.

ACKNOWLEDGMENTS

We thank J. Marko, C. Sorensen, and W. Stevenson for many useful discussions. This material is based upon work supported by the National Science Foundation under Grant No. OSR-9255223 (NSF-EPSCoR). This work also received matching support from the State of Kansas. Computations were carried out in the Sun-Sparcstation clusters at Kansas State University. The whole project required about one *Sparcstation-year* of CPU time.

[1] See, for example, D. H. Napper, *Polymeric Stabilization of Colloidal Dispersions* (Academic, London, 1983).
[2] W. B. Russel, D. A. Saville, and W. R. Schowalter, *Colloidal Dispersions* (Cambridge University Press, Cambridge, 1989).
[3] S. T. Milner, Science **251**, 905 (1991).
[4] A. Halperin, M. Tirrell, and T. P. Lodge, Adv. Polym. Sci. **100**, 31 (1991).
[5] H. J. Taunton, C. Toprakcioglu, L. J. Fetters, and J. Klein, Nature **332**, 712 (1988); Macromolecules **23**, 571 (1990); H. J. Taunton, C. Toprakcioglu, and J. Klein, *ibid.* **21**, 3333 (1988).
[6] A. N. Semenov, Zh. Eksp. Teor. Fiz. **88**, 1242 (1985) [Sov. Phys. JETP **61**, 733 (1985)].
[7] S. T. Milner, T. A. Witten, and M. E. Cates, Macromolecules **21**, 1610 (1988).
[8] S. Hirz, M. S. thesis, University of Minnesota, 1986; T. Cosgrove, T. Heath, B. van Lent, F. Leermakers, and J. Scheutjens, Macromolecules **20**, 1692 (1987); M. Muthukumar and J. S. Ho, *ibid.* **22**, 965 (1989).
[9] A. M. Skvortsov *et al.*, Polym. Sci. USSR **30**, 1706 (1988); E. B. Zhulina, V. A. Priamitsyn, and O. V. Borisov, Polym. Sci. USSR **31**, 205 (1989).
[10] S. Alexander, J. Phys. (Paris) **38**, 983 (1977).
[11] P. G. de Gennes, Adv. Colloid Interface Sci. **27**, 189 (1987); Macromolecules **13**, 1069 (1980).
[12] (a) A. Chakrabarti and R. Toral, Macromolecules **23**, 2016 (1990); (b) A. Chakrabarti, P. Nelson, and R. Toral, Phys. Rev. A **46**, 4930 (1992).
[13] P.-Y. Lai and K. Binder, J. Chem. Phys. **95**, 9288 (1991).
[14] M. Murat and G. S. Grest, Macromolecules **22**, 4054 (1989).
[15] P. Auroy, L. Auvray, and L. Leger, Phys. Rev. Lett. **66**, 719 (1991).

[16] P. Auroy, Y. Mir, and L. Auvray, Phys. Rev. Lett. **69**, 93 (1992).
[17] S. K. Satija, J. F. Anker, C. F. Majkrzak, T. Mansfield, G. Beaucage, R. S. Stein, D. R. Iyenger, T. J. McCarthy, and R. J. Composto (unpublished); T. Mansfield and S. K. Satija (private communications).
[18] C. Ligoure and L. Leibler, J. Phys. (Paris) **51**, 1313 (1990).
[19] S. Milner, Macromolecules **25**, 5487 (1992).
[20] P.-Y. Lai, J. Chem. Phys. **98**, 669 (1993).
[21] K. Kremer and K. Binder, Comp. Phys. Rep. **7**, 259 (1988).
[22] A. C. Balazs, M. Gempe, and C. W. Lantman, Macromolecules **24**, 168 (1991).
[23] M. T. Gurler, C. C. Crabb, D. M. Dahlin, and J. Kovac, Macromolecules **16**, 398 (1983).
[24] J. M. H. M Scheutjens and G. J. Fleer, J. Phys. Chem. **84**, 178 (1980).
[25] P. G. de Gennes, Macromolecules **13**, 1069 (1980).
[26] A. P. Gast and L. Leibler, Macromolecules **19**, 686 (1986).
[27] E. B. Zhulina, O. V. Borisov, and L. Bombacher, Macromolecules **24**, 4679 (1991); C. M. Wijmans, J. M. H. M. Scheutjens, and E. B. Zhulina, *ibid.* **25**, 2657 (1992).
[28] K. R. Shull, J. Chem. Phys. **94**, 5723 (1991).
[29] A. Budkowski, U. Steiner, J. Klein, and L. J. Fetters, Europhys. Lett. **20**, 499 (1992); M. Aubouy and E. Raphael, J. Phys. II (France) **3**, 443 (1993).
[30] Z. Gao and H. D. Ou-Yang, in *Colloid-Polymer Interactions,* edited by P. Dubin and P. Tong, Am. Chem. Soc. Symp. Ser. No. 532 (American Chemical Society, Washington, D.C., 1993).
[31] J. Klein *et al.*, Macromolecules **25**, 2062 (1992).

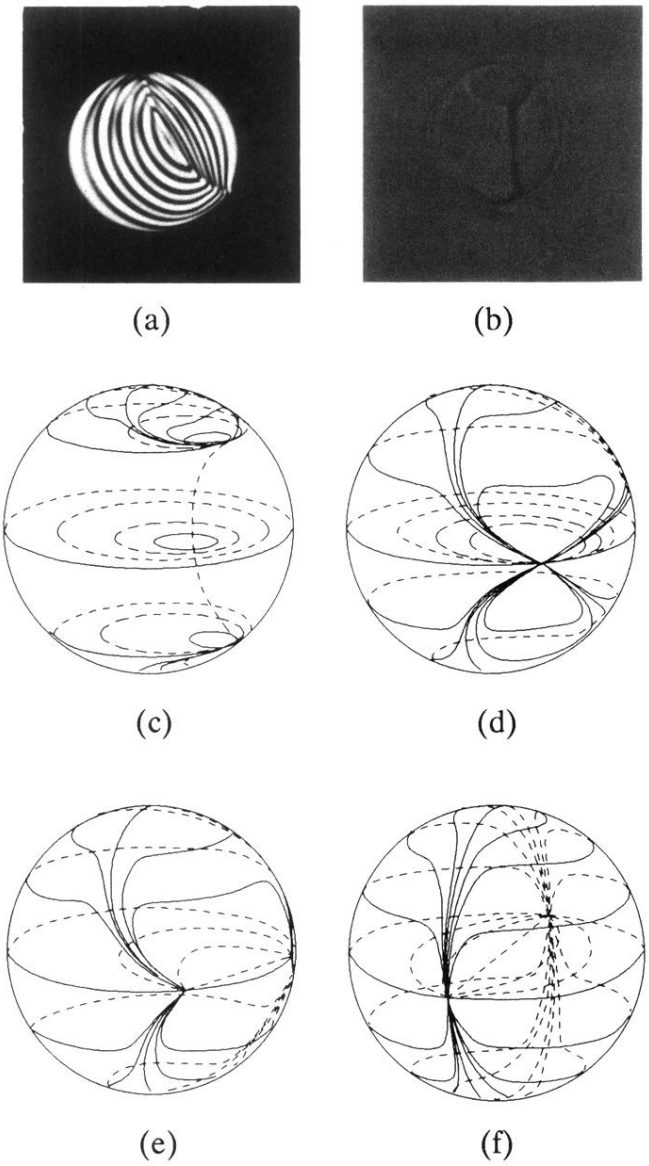

FIG. 9. (a),(b) Microscope photographs of instability in drops with axis parallel to **E** and $E = 667$ kV/m. (c)–(f) Explanation of instability transition from concentric to escaped planar bipolar structure. (c) $s = +1$ concentric boojums move toward each other causing escaped line to bend; (d) boojums combine to form single $s = +2$ boojum; (e) $s = +2$ boojum splits into two radial $s = +1$ boojums; (f) $s = +1$ boojums migrate to diametrically opposite positions to form escaped planar bipolar structure.